HHS Public Access

Author manuscript

Ann Biomed Eng. Author manuscript; available in PMC 2017 December 01.

Published in final edited form as:

Ann Biomed Eng. 2016 December ; 44(12): 3632–3644. doi:10.1007/s10439-016-1693-4.

Simvastatin Treatment Modulates Mechanically-Induced Injury and Inflammation in Respiratory Epithelial Cells

N. Higuita-Castro[1,3], **V.C. Shukla**[1,3], **C. Mihai**[1], and **S.N. Ghadiali**[1,2,3,*]

[1]Biomedical Engineering Department, The Ohio State University, Columbus, Ohio

[2]Department of Internal Medicine, Division of Pulmonary, Allergy, Critical Care and Sleep Medicine, The Ohio State University Wexner Medical Center, Columbus, Ohio

[3]Dorothy M. Davis Heart and Lung Research Institute, The Ohio State University Wexner Medical Center, Columbus, Ohio

Abstract

Mechanical forces in the respiratory system, including surface tension forces during airway reopening and high transmural pressures, can result in epithelial cell injury, barrier disruption and inflammation. In this study, we investigated if a clinically relevant pharmaceutical agent, Simvastatin, could mitigate mechanically induced injury and inflammation in respiratory epithelia. Pulmonary alveolar epithelial cells (A549) were exposed to either cyclic airway reopening forces or oscillatory transmural pressure *in vitro* and treated with a wide range of Simvastatin concentrations. Simvastatin induced reversible depolymerization of the actin cytoskeleton and a statistically significant reduction the cell's elastic modulus. However, Simvastatin treatment did not result in an appreciable change in the cell's viscoelastic properties. Simvastatin treated cells did exhibit a reduced height-to-width aspect ratio and these changes in cell morphology resulted in a significant decrease in epithelial cell injury during airway reopening. Interestingly, although very high concentrations (25–50 μM) of Simvastatin resulted in dramatically less IL-6 and IL-8 pro-inflammatory cytokine secretion, 2.5 μM Simvastatin did not reduce the total amount of pro-inflammatory cytokines secreted during mechanical stimulation. These results indicate that although Simvastatin treatment may be useful in reducing cell injury during airway reopening, elevated local concentrations of Simvastatin might be needed to reduce mechanically-induced injury and inflammation in respiratory epithelia.

Keywords

ventilation-induced lung injury; mechanotransduction; pressure-induced inflammation; mechanobiology; cell mechanics; power-law rheology

*Address for reprint requests and other correspondence: Samir N. Ghadiali, Professor, Director of Graduate Studies, Department of Biomedical Engineering, 270 Bevis Hall, 1080 Carmack Rd., Columbus, OH 43221, ghadiali.1@osu.edu, Phone: (614) 292-7742, Fax: (614) 292-7301.

Introduction

Mechanical forces in the respiratory system are a major determinate of epithelial cell injury and inflammation. For example, acute lung injury (ALI) involves disruption of the alveolar-capillary barrier and leads to heterogeneous fluid occlusion of pulmonary airway and alveoli. Although patients with ALI must be artificially ventilated for survival, this ventilation generates several pathological mechanical forces [1]. First, the over-distension of aerated regions results in abnormally large stretching forces on the epithelium which can cause cellular necrosis, barrier disruption, and secretion of pro-inflammatory cytokines [2–4]. Clinical trials [5] have demonstrated that this type of lung injury, known as volutrauma, can be prevented by using low tidal volumes protocols. Unfortunately, low volume ventilation can also cause significant lung injury and inflammation [6, 7] where the cyclic closure and reopening of fluid filled airways generates dynamic air-liquid interfacial stresses which can cause significant barrier disruption and plasma membrane rupture [8, 9]. Although elevated positive end expiratory pressure (PEEP) protocols have been used in an attempt to prevent this injury, known as atelectrauma, clinical trials have not definitively established that higher PEEP ventilation reduces lung injury [10, 11]. Interestingly, high PEEP protocols result in elevated levels of pro-inflammatory cytokines [12] and high transmural pressures can activate pro-inflammatory signaling pathways [13, 14]. Therefore, preventing the cellular injury and inflammation caused by pathological mechanical forces, including interfacial stresses and transmural pressure, is a major clinical need.

Several investigators have used combination of computational and experimental studies to investigate the pathological mechanisms responsible for cellular injury during atelectasis and airway reopening [7]. For example, using an in-vitro model of atelectrauma, Yalcin *et al.* [15] demonstrated that altering cytoskeletal mechanics could be used to reduce the amount of cell injury and detachment that occurs during airway reopening. Specifically, depolymerization of the actin cytoskeleton, resulted in more fluid-like epithelial cell that experienced less plasma membrane rupture and cell detachment. Continuum mechanics based computational models [16] indicate that this “fluidization”, i.e. an increase the power law structural dampening exponent (α), leads to dissipation of the applied interfacial stress and less cellular deformation/injury. Recently, we demonstrated that epithelial cells grown on compliant substrates are less susceptible to cellular injury during cyclic airway reopening [17]. In that study, the decreased injury susceptibility was due to morphological changes, where cells on softer substrates exhibit a decreased height-to-length aspect ratio, which according to computational studies [18], reduces the hydrodynamic stresses generated during airway reopening. Although changes in epithelial cell mechanics and morphology can modulate cell injury during airway reopening, it is not known if clinically relevant pharmaceuticals can be used to similarly modulate epithelial mechanics/morphology and the degree of cell injury during airway reopening.

In addition to physical injury (i.e. plasma membrane disruption and cell detachment), mechanical forces can also activate pro-inflammatory signaling in respiratory epithelia. For example, cyclic stretching results in pro-inflammatory cytokine secretion from alveolar epithelial cells [4] while fluid shear stress stimulates mucus secretion from respiratory epithelial cells [19]. Chronic and/or intermittent compressive stress is a potent stimulator of

mucin glycoprotein secretion in bronchial epithelial cells [20] and static and oscillatory pressures can also stimulate pro-inflammatory cytokine secretion from lung epithelial cells [13, 14]. Although modulation of the cytoskeleton has been shown to alter pressure-induced NF-κB activation [14], it is not known if clinically relevant pharmaceuticals can similarly modulate mechanically-induced inflammation in respiratory epithelia.

Statins are HMG-CoA reductase inhibitors that are commonly used to reduce serum cholesterol levels [21]. Statins also inhibit the synthesis of GTP-binding proteins involved in the Rho and Rac pathway, leading to pleotropic effects on stress fiber formation, cytoskeletal regulation and signal transduction [22]. Recently, investigators have shown that statins can reduce ventilation induced lung injury in rats and mice [23–25], prevent barrier disruption in isolated rabbit lungs ventilated with high pressure [26], and reduce lipopolysaccharide-induced pulmonary inflammation in healthy human volunteers [27]. However, a recently completed clinical trial [28] did not document improvements in clinical outcomes for patients with ALI. Therefore, more information is needed about the mechanisms by which statins alter cellular injury and inflammation during mechanical ventilation. Interestingly, Simvastatin has been shown to disrupt the actin cytoskeleton in cardiac fibroblasts and lung endothelial cells [29, 30] and similar cytoskeletal alterations in lung epithelial cells have been shown to alter the degree of mechanically-induced cell injury and inflammation [14, 15]. We therefore hypothesize that Simvastatin will alter the cytoskeletal mechanics and morphological properties of lung epithelial cells and that these changes in cell mechanics/morphology will alter both the degree of cell injury during airway reopening and the amount of mechanically-induced inflammation (i.e. pro-inflammatory cytokine secretion). We use both *in-vitro* models of epithelial cell injury and inflammation and biophysical characterization tools to test this hypothesis.

Materials and Methods

1. Cell Culture

Human alveolar epithelial cells (A549) (ATCC, Manassas, VA) were maintained in Dulbecco's Modified Eagle's Medium (DMEM) (Corning, Manassas, VA), supplemented with 10% Fetal Bovine Serum (FBS) (Thermo Scientific, Rockford, IL) and 1% of antibiotics/antimycotics mixture (Life Technologies, Grand Island, NY) at 37°C, 5% CO_2 and 95% relative humidity. Cells were seeded onto 40 mm diameter glass cover slips inside 60 mm petri dishes at a cell density of 3.6 x 10^4 cells/cm^2 and grown to confluence. Based on previous studies which treated lung epithelial or endothelial cells with 0.1 to 100μM Simvastatin [29, 31–33], in this study, A549 cells were incubated with 2.5 to 50μM Simvastatin (Cayman Chemical, Ann Arbor, MI) in supplemented media for 16–17 hours prior to each experiment and untreated cells were used as controls.

2. Fluid-filled airway reopening simulation

As described in our previous studies [17] and shown schematically in Fig 1, a Bioptechs FCS2 chamber (Bioptechs, Butler, PA) and a programmable PHD 2000 syringe pump (Harvard Apparatus, Holliston, MA) were used to expose cells to cyclic airway reopening conditions. Briefly, confluent samples were placed inside the chamber and the flow channel

(35mm length, 10mm width, and 0.5mm height) was filled with phosphate-buffered saline (PBS). PBS fluid was then removed from the channel at a constant flow rate to create an air-liquid interface that propagated over the epithelial monolayer at 3 mm/sec. The channel was re-filled and fluid removed five times to simulate the cyclic closure and reopening of fluid-filled airways. Cells were then stained using a live/dead cell viability assay (Life Technologies, Grand Island, NY) and imaged along the center of the channel via fluorescence microscopy at 10X (5–17 images per sample). For each image, the percentage of cell death was computed as the ratio of dead cells to total number of cells observed after 5 air-liquid propagations. Cell detachment was quantified as the difference between the number of cells present before and after the propagation of air-liquid interfaces relative to the number of cells before interface propagation. Cell counts were conducted using the Image J software (NIH, USA).

3. Characterization of Cytoskeletal structure

The effect of different Simvastatin concentrations on the actin cytoskeleton as well as the recovery of the cytoskeleton after removal of Simvastatin was assessed via fluorescence imaging. After 16 hours of treatment and/or 16 hours of treatment followed by 4–5 hours of recovery, cells were fixed with 10% Neutral Buffered Formalin (Thermo Scientific, Rockford, IL), permeabilized with a 0.1% Triton X-100 (Sigma-Aldrich, St. Louis MO), and incubated with a 0.1μM Alexa Fluor 488 Phalloidin (Invitrogen, Grand Island NY). Cell nuclei were counter stained with a 0.2 μg/mL DAPI (4',6-diamidino-2-phenylindole) (Sigma-Aldrich, St. Louis MO) and an Olympus IX-81 inverted microscope was used to image the cytoskeleton.

4. Characterization of cell morphology and mechanics

Atomic force microscopy (AFM) was used to investigate the effect of Simvastatin therapy on lung epithelial cell morphology and mechanics. A Bioscope II AFM (Digital Instruments, Santa Barbara CA) mounted on the stage of an Axiovert 200 inverted optical microscope (Zeiss, Germany) was used to obtain measurements for cells cultured on glass cover slips and maintained in CO2-independent media (Life Technologies, Grand Island, NY). Silicon nitride cantilevers with a nominal spring constant k = 0.01 N/m, length of 200 μm, and a regular four-sided pyramidal tip with an angle θ= 35° were used for these measurements (Veeco, Santa Barbara CA). Following protocols previously reported by our group [17, 34], 5–12 regions per sample were scanned in contact mode and the deflection error and height image was recorded. Height images were analyzed with the NanoScope Analysis software package (Bruker Instruments, Camarillo CA) to measure cell height, width and length. Here, length was defined as the largest edge-to-edge distance and width as the maximum edge-to-edge distance perpendicular to the length axis. The aspect ratio of the cells was determined in terms of height- to-length and height-to-width ratios. AFM height images were also used to calculate the volume of untreated and Simvastatin treated cells. The volume of individual cells (V) was calculated by integrating the height measurements over the area of the cell (Eqn. 1):

$$V=\int_{cell} H\, dA=(\sum_{i=1}^{n} H_i) * dA_i \quad (1)$$

where H_i represents height measurements for a given cell consisting of n pixels and dA_i is the area of each pixel unit. All the height images were captured at resolution of 256x256 pixels for an area of 50μm x50μm.

Next, under contact mode the AFM tip was moved toward the cell and the resulting tip deflection (d) as a function of vertical position (z) was recorded. Four to five 50μm x 50μm regions were scanned per sample and an average of 130 z vs. d curves were recorded per region at a specific indentation (δ). As described previously [17], the Young's modulus (E) and the z- position where the cantilever tip contacts the cell surface (zc) were then estimated by fitting the raw z vs. d data with a modified Hertz model assuming incompressibility. Data analysis was restricted to the lower region of the force curve (0.05–0.5nN) to avoid noise in the <0.05nN range and nonlinearities associated with deep indentations.

Finally, a previously described oscillatory AFM technique [17, 35] was used to investigate if Simvastatin therapy altered the viscoelastic properties of A549 cells. Briefly, at each cell surface location, standard z vs. d curves were obtained to measure E and zc and indent the cells by a known value, δ_0. The cantilever was then oscillated in the z-direction at a given frequency, f, and the magnitude (m_d) and phase shift (Φ_d) of the deflection signal was recorded. Taylor series expansions and Fourier transforms were used to obtain a frequency domain Hertz model that accounts for viscous drag between the cantilever and surrounding liquid.

$$G*(\omega)=\frac{1-\nu}{3\delta_o \tan\theta}\left(\frac{k*d(\omega)}{\delta(\omega)}-i\omega b(0)\right) \quad (2)$$

Here G*(ω) is the complex shear modulus, ω=2π*f*, *d*(ω) is defined as $d(\omega)=m_d*\exp(i[\omega t+\Phi_d])$, δ (ω) is defined as $\delta(\omega)=z(\omega)-z_c-d(\omega)$ where z(ω) is defined as the Fourier transforms of z and b(0) is the drag coefficient. We assumed a Poisson's ratio ν =0.5 and calculated b(0) for each AFM tip. Eqn. (2) was used to obtain measurements of G* for frequencies in the range *f* = 5–160 Hz and the resulting G* vs. ω curves were analyzed with a power-law structural dampening model [36].

$$G*(\omega)=G_o(1+i\eta)\left(\frac{\omega}{\omega_0}\right)^{\alpha}+i\omega\mu \quad (3)$$

Here G_0 is the value of the storage modulus at ω_o, ω_o is a reference frequency (set to 31.4 rads/s), α is the power-law exponent, $\eta=\tan(\alpha\pi/2)$, and μ is the Newtonian viscous damping coefficient. A least squared regression with Eqn. (3) was used to obtain values for G_0, α and μ where G_0 represents the effective cell stiffness and α is a measure of the cell's

viscoelasticity where $\alpha=0$ represents a purely elastic material and increases in α represent increased fluidity [15].

5. Pressure-Induced Inflammation

Although accurate assessment of inflammation after airway reopening experiments were not possible due to significant cell detachment, we used a previously described oscillatory pressure-induced model of inflammation [13] to investigate how Simvastatin treatment influences pro-inflammatory cytokine secretion during mechanical stimulation. For these studies, A549 cells were seeded on the apical compartment of 24 mm polyester Transwell permeable supports (Corning, Tewksbury, MA) at a cell density of 2.6×10^4 cells/cm^2. Cells were cultured under an air-liquid interface and after 24 hours the cells were treated with Simvastatin for 16–17 hours in complete media. Cells were then exposed to 20 cmH_2O of oscillatory pressure at 0.2Hz for 12 hours. This pressure magnitude was selected based on typical pressure values observed during mechanical ventilation [11]. Media from the basal compartment was collected and ELISA sets from BD Biosciences (San Jose, CA) were used to measure human IL-6 and IL-8 cytokine concentration following the vendor's protocol.

6. Statistical analysis

All data were tested for normality using a Shapiro-Wilk test. Data that followed a normal distribution were analyzed using a one-way or two-way analysis of variance (ANOVA) with post-hoc least significant difference test and reported as mean ± standard error. Data that were not normally distributed were analyzed using non-parametric statistical analysis, i.e. ANOVA on ranks with post-hoc Mann-Whitney Rank Sum test, and reported as box and whisker plots or median with 25/75 percentile.

Results

1. Simvastatin alters Cytoskeletal Structure

As shown in Fig 2A–F, 16 hours of Simvastatin treatment induced dose dependent depolymerization of the actin cytoskeleton. For 2.5 to 10μM Simvastatin treatment, we observed modest alterations in the actin cytoskeleton but actin stress fibers can still be seen distributed throughout the cytoplasm. Conversely, higher concentrations (25 and 50μM) resulted in significant disruption of the actin cytoskeleton and loss of actin stress fibers. High concentrations also resulted in more punctuate actin staining patterns. Interestingly, as shown in Fig 2G–H, these disruptions in the cytoskeleton were reversible upon removal of Simvastatin treatment. Specifically, cells initially treated with 16 hours of 25 μM Simvastatin exhibited significant re-polymerization of actin filaments 4 hours after removal of Simvastatin treatment and further improvements in cytoskeletal structure after 5 hours.

2. Simvastatin Mitigates Cellular Injury during Cyclic Airway Reopening

As shown in Fig 3, consistent with previous studies [15, 37], cyclic airway reopening results in significant cell death and detachment in untreated/control A549 cells where we observed 28% median cell death and 23% median cell detachment after 5 reopening events. Interestingly, Simvastatin treated epithelial monolayers presented a statistically significant, dose-dependent decrease in epithelial cell death and detachment after 5 reopening events

(Fig. 3). Specifically, treatment with 2.5μM to 50μM Simvastatin resulted in 65% to 85% decrease in cell death and a 47% to 91% decrease in cell detachment over control values. The median cell death and detachment at all Simvastatin concentrations was significantly lower than the median values of cell death and detachment under control conditions ($p<0.05$). In addition, the median cell death values at 25and 50μM Simvastatin (5.9% and 4.4%, respectively) were significantly lower than the median cell death value at 2.5μM (9.8%). The median cell detachment values at 25 and 50μM Simvastatin (3.0% and 2.0%, respectively) were also significantly lower than the median cell detachment a 2.5μM (11.9%). Although all doses of Simvastatin significantly reduced cell death and detachment in comparison with non-treated cells, the difference between Simvastatin doses was not significant for concentrations above 25μM.

3. Effect of Simvastatin on cell mechanics and morphology

AFM characterization (Figs 4, 5 and 6) indicate that Simvastatin treatment had a dose dependent effect on the morphological and mechanical properties of lung epithelial cells. First, as shown in Fig 4A, AFM indentation experiments indicate that untreated A549 cells had a median Young's modulus of 1.56KPa and that 2.5μM Simvastatin treatment resulted in a minor decrease in the median Young's modulus to 1.48KPa ($p=0.05$) while treatment with 25μM Simvastatin resulted in a larger and more significant ($p<0.01$) decrease in Young's modulus (1.09KPa). As shown in Fig 4B, the Young's modulus distribution in both untreated and Simvastatin treated samples were not normally distributed but treatment with increasing dosage of Simvastatin results in a clear shift of the Young's modulus distribution to lower values.

Oscillatory AFM techniques were used to measure the complex shear modulus, G*, as a function of frequency (ω) at ~80 cell surface locations per sample and an example of this data at each Simvastatin concentration is shown in Fig 5B. A regression analysis with Eqn. (3) (see solid lines in Fig 5B), was then used to determine the reference shear modulus, G_0, the power-law exponent, α, and the Newtonian viscous damping coefficient μ. As shown in Figure 5A, Simvastatin treatment resulted in a statistically significant ($p<0.01$) 33%–38% decrease in G_0. However, Simvastatin treatment did not have a pronounced effect on α or μ. First, although treatment with 2.5μM Simvastatin did result in a statistically significant increase in the median value of α ($p=0.03$), the magnitude of this increase was minor where the median α value was 0.12 and 0.14 for control and 2.5μM Simvastatin treated cells respectively. Furthermore, the median value of α in 5.0μM Simvastatin treated cells, 0.11, was not statistically different than the control value ($p=0.375$). The median values for μ under control, 2.5 and 5.0μM Simvastatin conditions were 0.90, 0.75 and 0.69 Pa*s respectively and ANOVA on ranks indicated that these median values were not statistically different ($p=0.631$).

Finally, AFM was used to measure the morphology of control and Simvastatin treated cells. As shown in Fig 6A, representative AFM height images indicate that cells treated with 2.5μM and 25μM Simvastatin exhibit a more flatten morphology as compared to control untreated cells. Quantitative analysis of these images indicate that Simvastatin treated cells exhibit a statistically significant decrease in cell height (mean height of 3.0μm and 2.7μm for

cells treated with 2.5 and 25μM Simvastatin, respectively) in comparison with non-treated cells (mean height of 3.7μm) ($p<0.05$) (Fig. 6B). No significant changes in cell width or length were observed for cells treated with Simvastatin in comparison with control cells. As a result, Simvastatin treatment resulted in a statistically significant ($p<0.05$) decrease in the height-to-width ratio (mean height-to-width ratios of 0.15, 0.12 and 0.09 in control, 2.5 and 25μM samples respectively). Similarly, we observed a statistically significant ($p<0.05$) decrease in the height-to-length ratio in cells treated with 25μM Simvastatin and a trend towards a lower height-to-length ratio in cells treated with 2.5μM Simvastatin (height/length ratios of 0.11, 0.09 and 0.07 in control, 2.5 and 25μM samples respectively). Interestingly, as shown in the Fig 6D treating cells with either 2.5 or 25μM Simvastatin did not result in a statistically significant change in overall cell volume.

4. Effect of Simvastatin on Pressure Induced Inflammation

As shown in Figure 7AB, Simvastatin treatment resulted in dose-dependent changes in IL-6 and IL-8 pro-inflammatory cytokine secretion during mechanical stimulation. First, consistent with previous studies [13], 12 hours of oscillatory pressure resulted in a statistically significant ($p<0.01$) increase in IL-6 and IL-8 secretion in untreated A549 cells. Two-way ANOVA indicates that both Simvastatin concentration and pressure-stimulation were significant factors ($p<0.01$). For Simvastatin concentrations ≤10μM, 12 hours of pressure induced a statistically significant ($p<0.01$) increase in IL-6 and IL-8 secretion relative to cells exposed to no pressure at the same Simvastatin concentration. However, at higher concentrations (25 and 50μM), 12 hours of pressure stimulation did not result in a statistically significant change in IL-6 and IL-8 secretion. Considering only samples simulated with 12 hours of pressure, IL-6 concentrations in the 2.5μM treated cells were statistically higher ($p<0.01$) than the IL-6 concentration in untreated cells. In contrast, after 12 hours of pressure stimulation, IL-6 concentrations in the 10, 25 and 50μM treated cells were statistically lower ($p<0.01$) than the concentration in untreated cells. Similarly, after 12 hours of pressure stimulation, IL-8 concentrations were statistically ($p<0.01$) higher in cells treated with 2.5 and 5μM Simvastatin and statistically lower for high dose Simvastatin treatment (25 or 50μM). Although the data in Figure 7A indicates that Simvastatin alters the amount of IL-6 and IL-8 cytokine secretion after 12 hours of pressure stimulation, it is also clear that Simvastatin alters the baseline level of cytokine secretion under no pressure conditions. Therefore, to investigate how Simvastatin alters the relative change in IL-6 and IL-8 cytokine secretion during pressure stimulation, in Figure 7B we report the fold-change in cytokine levels as a function of Simvastatin concentration. A one-way ANOVA indicates that a all Simvastatin concentrations reduces the relative increase in IL-6 and IL-8 secretion due to pressure stimulation ($p<0.01$) with the greatest reduction at high dosage. We conclude that although all concentrations of Simvastatin reduce the relative amount of pressure induced pro-inflammatory cytokine secretion, high dosages of Simvastatin (25 to 50μM) is required to reduce the total amount of IL-6 and IL-8 secretion during mechanical stimulation.

Discussion

Simvastatin is a commonly prescribed pharmaceutical used to control serum cholesterol levels [21]. Simvastatin also has pleotropic effects and may play a role in regulating ventilation induced lung injury [23–25]. For example, Simvastatin has been shown to mitigate lung injury and inflammation caused by lung overdistension during high tidal volume ventilation [23–25]. However, it is not known if Simvastatin can mitigate cellular injury and inflammation during low tidal volume ventilation. At low lung volumes, the cyclic closure and reopening of fluid-airways results in significant cellular injury and barrier disruption [6, 7]. In addition, ventilation at higher pressures has also been shown to elicit a pro-inflammatory response both in-vivo [12] and in-vitro [13, 14]. Therefore, the goal of this study was to investigate if Simvastatin can alter the mechanotransduction processes responsible for cellular injury during airway reopening and pressure-induced inflammation in lung epithelia.

Previous studies indicate that 16 hours of Simvastatin treatment results in disruption of the actin cytoskeleton and a loss of actin stress fibers in lung microvascular endothelial cells [29, 32]. Consistent with these previous studies, our data (Fig. 2) indicates that 16 hours of Simvastatin treatment also disrupts the actin cytoskeleton in A549 lung epithelial cells in a dose-dependent fashion. 2.5 to 10 μM Simvastatin treatment resulted in modest cytoskeletal alterations and some loss of actin stress fibers while higher concentrations (25 and 50μM) resulted in a significant loss of actin stress fibers. Interestingly, changes in cytoskeletal structure were reversible where cells initially treated with 25μM Simvastatin exhibited increased actin stress fiber formation 4–5 hours after of removal of Simvastatin. Since an intact actin cytoskeleton may be required for efficient wound repair following lung injury [38], the reversibility of Simvastatin's effect on the actin cytoskeleton may have important clinical implications.

As shown in Fig 3, Simvastatin treatment also reduced the amount of cell injury (i.e. cell death and detachment) after 5 reopening events. Interestingly, compared to untreated samples, treatment with 2.5 and 5.0μM Simvastatin resulted in a large decrease in cell injury while higher concentrations (25 and 50μM) resulted in modestly lower amount of cell injury compared to the 2.5μM condition. This result indicates that although high concentrations of Simvastatin provide the greatest reduction in cell injury, 2.5μM of Simvastatin is also effective at reducing the physical injury caused by cyclic airway closure and reopening. To determine the biomechanical mechanisms of reduced cell injury following Simvastatin treatment, we investigated how Simvastatin alters the biomechanical and morphological properties of A549 cells. Since previous experimental and computational studies [15, 16] indicate that increases in the cell's power-law exponent (α) can reduce the amount cell injury during reopening, we conducted oscillatory AFM experiments to investigate if Simvastatin alters the power-law rheology of A549 cells. As shown in Fig 5, Simvastatin treatment did not result in an appreciable change in α or the Newtonian viscosity μ and therefore changes in viscoelasticity cannot be used to explain the decreased cell injury and detachment observed at 2.5 and 5.0μM. In addition, AFM measurements of Young's modulus (Fig 4) and reference storage modulus (Fig 5A) indicate that Simvastatin treatment results in a statistically significant decrease in cell stiffness. However, computational models

[39] indicate that for constant hydrodynamic loading, this decrease in cell stiffness alone would lead to increased plasma membrane strain and thus more injury. Therefore, changes in the cell's elastic properties cannot be used to explain decreased cell injury with Simvastatin treatment.Finally, AFM was used to quantify how Simvastatin therapy alters the morphology of A549 cells. As shown in Fig 6, treatment with 2.5 and 25μM resulted in a significant dose dependent decrease in the cell's height/width and height/length aspect ratio. A computational study by Jacob & Gaver [18] indicates that this decrease in aspect ratio would significantly reduce the hydrodynamic stresses exerted on airway epithelial cells during reopening. In addition, computational studies by Dailey et al [39] indicate that cells with a smaller aspect ratio experience less plasma membrane strain even if hydrodynamic forces are constant. Together, these computational studies predict that cells with decreased aspect ratios would experience less cell injury during airway reopening. Consistent with this prediction, the experimental results in Figs. 3 & 6 indicate that Simvastatin treatment results in cells with a reduced aspect ratio and less cell injury.

Although Simvastatin treatment reduces the maximum cell height (Fig 6B), it does not change the cell volume even for a preserved cell length and width. This change in morphology is consistent with a "flattening" of the cell topography as shown in the schematic in Fig 6E where untreated cells have a large height and significant topological variation while Simvastatin treated cells are "flattened" with a reduced height and topological variation. Note that in this schematic the shaded area for both cells is equivalent and thus the volume has not changed. Interestingly, this reduction in topological variation is very similar to the conditions simulated numerically by Jacob and Gaver [18]. That study found that cells with a reduced topological variation experience a significant reduction hydrodynamic stress from the air-liquid interface. Since independently reducing interfacial and hydrodynamic stress via the addition of a pulmonary replacement surfactant (Infasurf) has already been shown to reduce cell injury [37], the stress reduction associated with a reduced aspect ratio is consistent with the reduced cell injury observed in Simvastatin treated cells. We conclude that a reduction in cell height, which in-turn reduces the hydrodynamic stresses on the cell membrane may be the critical factor in reducing cellular injury during Simvastatin treatment. Although Simvastatin has anti-inflammatory properties and has been shown to regulate inflammation due to lung over-distension [24], in this study we investigated if Simvastatin could also mitigate pressure-induced inflammation in lung epithelia. Consistent with previous studies [12–14], 12 hours of cyclic pressure induced a significant increase in IL-6 and IL-8 pro-inflammatory secretion from A549 cells.

Although Simvastatin treatment reduced the relative increase IL-6 in IL-8 secretion due to mechanical stimulation (Fig 7CD), Simvastatin treatment also altered the baseline levels of IL-6 and IL-8 secretion (Fig 7AB). As a result, 2.5 to 5 μM Simvastatin treatment actually lead to a higher amount of cytokine in the media following mechanical stimulation. Conversely, at higher Simvastatin concentrations (25 and 50μM), cytokine concentrations in the media following mechanical stimulation were remarkably reduced. We conclude that although Simvastatin may reduce the relative amount of pressure-induced inflammation, very high dosages of Simvastatin may be needed to reduce the absolute amount of pressure-induced cytokine secretion.

Although this in-vitro study indicates that Simvastatin can be used to prevent cellular injury during airway reopening, a recent multi-center clinical study [28] indicates that high oral dosage of Simvastatin (80 mg/day) does not reduce the number of ventilator free days or mortality. Interestingly, although the Simvastatin concentrations used in this study (2.5–50 μM) is consistent with previous in-vitro studies [29, 31–33], pharmacokinetic studies [40] indicate that 40 mg/day Simvastatin therapy yields a maximum plasma concentration of ~0.2 μM. Since this study indicates that 2.5 μM of Simvastatin can reduce cell injury/detachment during airway reopening, techniques that locally increase drug concentration at the lung epithelium might be needed to see a clinical benefit. We note that simply increasing the oral dose over 80 mg/day is not clinically viable due to the well-known myotoxic effects of statins [41] and therefore techniques that only deliver Simvastatin to the lung epithelium, i.e. aerosolized drug delivery, may be needed to achieve high local concentrations in the lung.

As with all in-vitro studies, there are some limitations that could be further addressed in future studies. First, the current study utilized a transformed lung epithelial cell line and future studies could investigate if Simvastatin therapy also protects primary human airway epithelial cells from injury during airway reopening. Future studies could also investigate if Simvastatin influence plasma membrane injury and repair in other wounding systems relevant to ventilation induced lung injury, i.e. stretching deformations. In addition, future studies could investigate if different statin preparations, e.g. atorvastatin or rosuvastatin, also have pleotropic effects on cell injury/inflammation during airway reopening. Although this study cultured cells on a rigid glass surface, a recent study by our group investigated how changes in substrate stiffness influence cellular injury during compliant airway reopening and future studies could use similar systems to investigate if Simvastatin therapy reduces cellular injury during compliant airway reopening. Finally, in this study we demonstrated that cells with a decreased aspect ratio experience less cell injury during reopening and that this experimental results is consistent with previous computational predictions [18, 39]. However, those computational studies assumed rigid or elastic cells and therefore future studies could incorporate more complex viscoelastic or poroelastic material properties to further confirm the effect of aspect ratio on cell injury.

In summary, we have demonstrated that Simvastatin treatment alters the structural, biomechanical and morphological properties of lung epithelial cells. In addition, 2.5 to 5μM Simvastatin therapy was very effective at reducing the amount of cellular injury and detachment during cyclic airway reopening. Results indicate that morphological changes in lung epithelial cells, i.e. a reduced cell height, during Simvastatin treatment may be the primary mechanisms for cytoprotection during airway reopening. We also demonstrated that Simvastatin can reduce the relative amount of pressure-induced pro-inflammatory cytokine production from lung epithelial cells. However, dramatic reductions in the absolute amount of cytokine production were only observed for very high Simvastatin concentrations, 25 to 50μM. Therefore, these studies suggest that although Simvastatin might be an effective way to prevent atelectruama during mechanical ventilation, higher local concentrations may be required to prevent ventilation induced lung inflammation.

Acknowledgments

This work was supported in part by AHA 60030975, NIH P50DC007667 and NSF 0852417.

References

1. Suki B, Hubmayr R. Epithelial and endothelial damage induced by mechanical ventilation modes. Curr Opin Crit Care. 2014; 20(1):17–24. [PubMed: 24300621]
2. Cavanaugh KJ, Cohen TS, Margulies SS. Stretch increases alveolar epithelial permeability to uncharged micromolecules. Am J Physiol Cell Physiol. 2006; 290(4):C1179–88. [PubMed: 16282193]
3. Tschumperlin DJ, Oswari J, Margulies AS. Deformation-induced injury of alveolar epithelial cells. Effect of frequency, duration, and amplitude. Am J Respir Crit Care Med. 2000; 162(2 Pt 1):357–62. [PubMed: 10934053]
4. Vlahakis NE, et al. Stretch induces cytokine release by alveolar epithelial cells in vitro. Am J Physiol. 1999; 277(1 Pt 1):L167–73. [PubMed: 10409244]
5. The Acute Respiratory Distress Syndrome Network. Ventilation with lower tidal volumes as compared with traditional tidal volumes for acute lung injury and the acute respiratory distress syndrome. N Engl J Med. 2000; 342(18):1301–8. [PubMed: 10793162]
6. D'Angelo E, et al. Cytokine release, small airway injury, and parenchymal damage during mechanical ventilation in normal open-chest rats. J Appl Physiol. 2008; 104(1):41–9. [PubMed: 17962576]
7. Ghadiali SN, Gaver DP. Biomechanics of liquid-epithelium interactions in pulmonary airways. Respir Physiol Neurobiol. 2008; 163(1–3):232–43. [PubMed: 18511356]
8. Hussein O, et al. Biophysical determinants of alveolar epithelial plasma membrane wounding associated with mechanical ventilation. Am J Physiol Lung Cell Mol Physiol. 2013; 305(7):L478–84. [PubMed: 23997173]
9. Douville NJ, et al. Combination of fluid and solid mechanical stresses contribute to cell death and detachment in a microfluidic alveolar model. Lab Chip. 2011; 11(4):609–19. [PubMed: 21152526]
10. Briel M, et al. Higher vs lower positive end-expiratory pressure in patients with acute lung injury and acute respiratory distress syndrome: systematic review and meta-analysis. JAMA. 2010; 303(9):865–73. [PubMed: 20197533]
11. Brower RG, et al. Higher versus lower positive end-expiratory pressures in patients with the acute respiratory distress syndrome. N Engl J Med. 2004; 351(4):327–36. [PubMed: 15269312]
12. Hong CM, et al. Low tidal volume and high positive end-expiratory pressure mechanical ventilation results in increased inflammation and ventilator-associated lung injury in normal lungs. Anesth Analg. 2010; 110(6):1652–60. [PubMed: 20103541]
13. Huang Y, et al. miR-146a regulates mechanotransduction and pressure-induced inflammation in small airway epithelium. FASEB J. 2012; 26(8):3351–64. [PubMed: 22593544]
14. Huang Y, Haas C, Ghadiali SN. Influene of Transmural Pressure and Cytoskeletal Structure on NF-KB Activation in Respiratory Epithelial Cell. Cellular and Molecular Bionengineering. 2010; 3(4): 415–427.
15. Yalcin HC, et al. Influence of cytoskeletal structure and mechanics on epithelial cell injury during cyclic airway reopening. Am J Physiol Lung Cell Mol Physiol. 2009; 297(5):L881–91. [PubMed: 19700641]
16. Dailey HL, Ghadiali SN. Influence of power-law rheology on cell injury during microbubble flows. Biomech Model Mechanobiol. 2010; 9(3):263–79. [PubMed: 19865840]
17. Higuita-Castro N, et al. Influence of airway wall compliance on epithelial cell injury and adhesion during interfacial flows. J Appl Physiol (1985). 2014; 117(11):1231–42. [PubMed: 25213636]
18. Jacob AM, Gaver DP. An investigation of the influence of cell topography on epithelial mechanical stresses during pulmonary airway reopening. Physics of Fluids. 2005; 17(3)
19. Even-Tzur N, et al. Mucus secretion and cytoskeletal modifications in cultured nasal epithelial cells exposed to wall shear stresses. Biophys J. 2008; 95(6):2998–3008. [PubMed: 18487304]

20. Park JA, Tschumperlin DJ. Chronic intermittent mechanical stress increases MUC5AC protein expression. Am J Respir Cell Mol Biol. 2009; 41(4):459–66. [PubMed: 19168703]
21. Collaborators CTTC, et al. The effects of lowering LDL cholesterol with statin therapy in people at low risk of vascular disease: meta-analysis of individual data from 27 randomised trials. Lancet. 2012; 380(9841):581–90. [PubMed: 22607822]
22. Wang CY, Liu PY, Liao JK. Pleiotropic effects of statin therapy: molecular mechanisms and clinical results. Trends Mol Med. 2008; 14(1):37–44. [PubMed: 18068482]
23. Zhao W, Song H, Huo W. Long-term administration of simvastatin reduces ventilator-induced lung injury and upregulates heme oxygenase 1 expression in a rat model. J Surg Res. 2015; 199(2):601–7. [PubMed: 26163326]
24. Muller HC, et al. Simvastatin attenuates ventilator-induced lung injury in mice. Crit Care. 2010; 14(4):R143. [PubMed: 20673352]
25. Manitsopoulos N, et al. Inhibition of HMGCoA reductase by simvastatin protects mice from injurious mechanical ventilation. Respir Res. 2015; 16:24. [PubMed: 25848815]
26. Siempos, et al. Pretreatment with atorvastatin attenuates lung injury caused by high-stretch mechanical ventilation in an isolated rabbit lung model. Crit Care Med. 2010; 38(5):1321–8. [PubMed: 20308883]
27. Shyamsundar M, et al. Simvastatin decreases lipopolysaccharide-induced pulmonary inflammation in healthy volunteers. Am J Respir Crit Care Med. 2009; 179(12):1107–14. [PubMed: 19324974]
28. McAuley DF, et al. Simvastatin in the acute respiratory distress syndrome. N Engl J Med. 2014; 371(18):1695–703. [PubMed: 25268516]
29. Chen W, et al. Endothelial cell barrier protection by simvastatin: GTPase regulation and NADPH oxidase inhibition. Am J Physiol Lung Cell Mol Physiol. 2008; 295(4):L575–83. [PubMed: 18658277]
30. Copaja M, et al. Simvastatin disrupts cytoskeleton and decreases cardiac fibroblast adhesion, migration and viability. Toxicology. 2012; 294(1):42–9. [PubMed: 22306966]
31. Wu Y, et al. Restoration of alveolar type II cell function contributes to simvastatin-induced attenuation of lung ischemia-reperfusion injury. Int J Mol Med. 2012; 30(6):1294–306. [PubMed: 23076613]
32. Jacobson JR, et al. Cytoskeletal activation and altered gene expression in endothelial barrier regulation by simvastatin. Am J Respir Cell Mol Biol. 2004; 30(5):662–70. [PubMed: 14630613]
33. Zeki AA, et al. Differential effects of simvastatin on IL-13-induced cytokine gene expression in primary mouse tracheal epithelial cells. Respir Res. 2012; 13:38. [PubMed: 22583375]
34. Mihai C, et al. PTEN inhibition improves wound healing in lung epithelia through changes in cellular mechanics that enhance migration. Am J Physiol Lung Cell Mol Physiol. 2012; 302(3):L287–99. [PubMed: 22037358]
35. Alcaraz J, et al. Microrheology of human lung epithelial cells measured by atomic force microscopy. Biophys J. 2003; 84(3):2071–9. [PubMed: 12609908]
36. Fabry B, et al. Scaling the microrheology of living cells. Physical Review Letters. 2001; 8714(14)
37. Bilek AM, Dee KC, Gaver DP 3rd. Mechanisms of surface-tension-induced epithelial cell damage in a model of pulmonary airway reopening. J Appl Physiol (1985). 2003; 94(2):770–83. [PubMed: 12433851]
38. Crosby LM, Waters CM. Epithelial repair mechanisms in the lung. Am J Physiol Lung Cell Mol Physiol. 2010; 298(6):L715–31. [PubMed: 20363851]
39. Dailey HL, et al. Image-based finite element modeling of alveolar epithelial cell injury during airway reopening. J Appl Physiol. 2009; 106(1):221–32. [PubMed: 19008489]
40. Cheng H, et al. Influence of age and gender on the plasma profiles of 3-hydroxy-3-methylglutaryl-coenzyme A (HMG-CoA) reductase inhibitory activity following multiple doses of lovastatin and simvastatin. Pharm Res. 1992; 9(12):1629–33. [PubMed: 1488408]
41. Tomaszewski M, et al. Statin-induced myopathies. Pharmacol Rep. 2011; 63(4):859–66. [PubMed: 22001973]

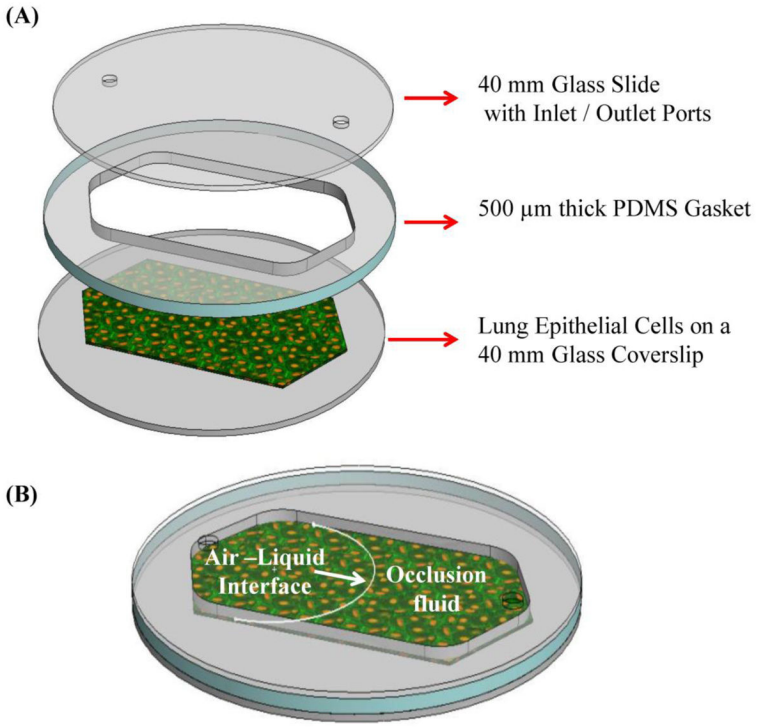

Figure 1.

(A) Schematic representation of the Bioptechs FCS2 chamber used to simulate fluid filled airway reopening, and (B) schematic representation of airway reopening simulation.

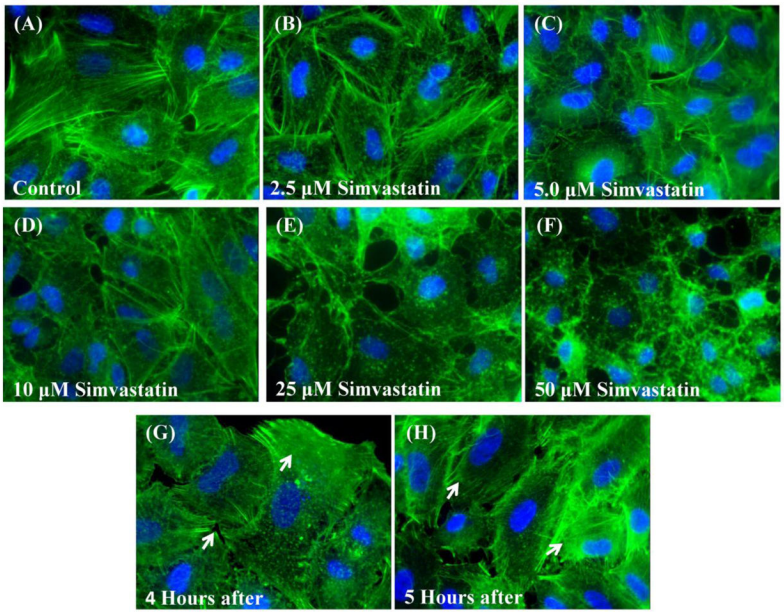

Figure 2.

Simvastatin treatment alters the actin cytoskeleton in A549 cells in a dose dependent fashion. (A)–(F) A549 cells on glass after 16–17 hours of treatment with different Simvastatin concentrations. (E&F) Recovery of the cell's actin cytoskeleton as indicated by the presence of stress fibers (white arrows) 4 and 5 hours after treatment with 25 µM Simvastatin (Actin – green, Nuclei – blue, 60X).

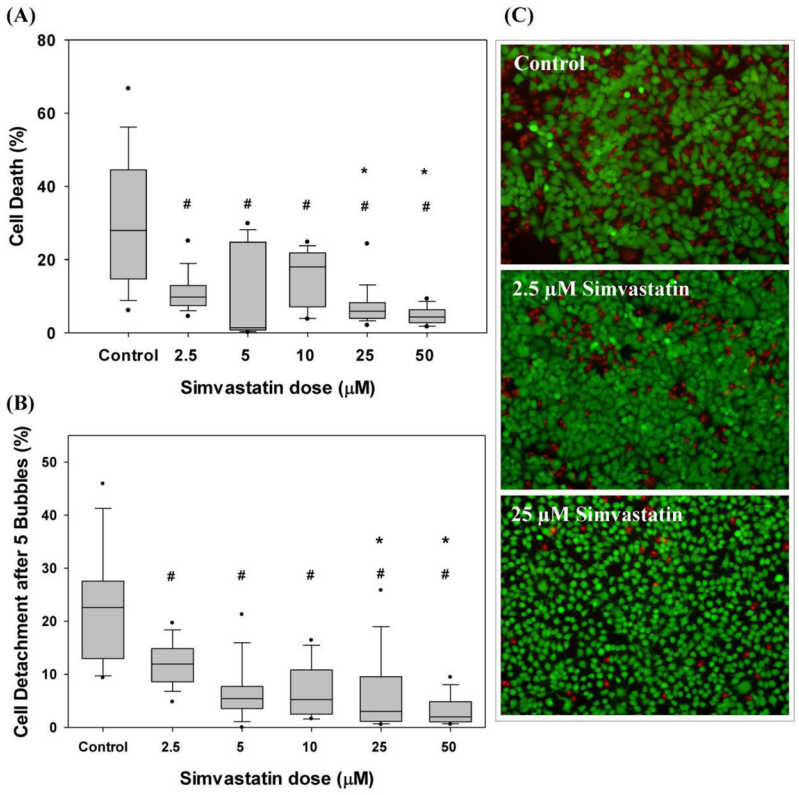

Figure 3.

Dose dependent effect of Simvastatin on (A) cell injury and (B) cell detachment after 5 airway reopening simulations. # Indicates significant difference with respect to control conditions ($p<0.01$) and * indicates significant difference with respect to injury/detachment at 2.5uM ($p<0.01$). Data analyzed via ANOVA on Ranks and post-hoc Mann-Whitney Rank Sum Tests. N= 2–5 experiments with 5–17 images per sample. (C) Representative images of live and dead fluorescent imaging after airway reopening (green: live cells, red: dead cells)

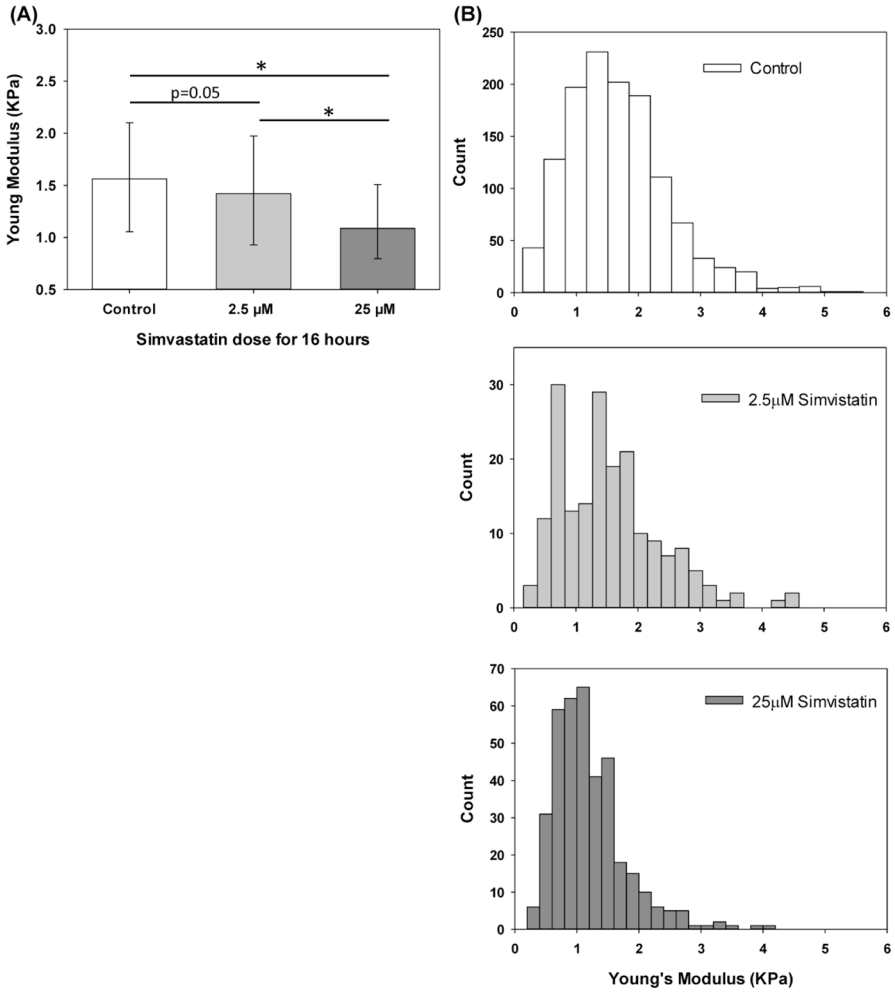

Figure 4.

Dose-dependent effect of Simvastatin on the Young's modulus of A549 cells. A) Median with 75/25% values of Young Modulus's measured via AFM in control, 2.5 and 25μM samples. B) Histograms of AFM Young's Modulus measurements. * Indicates significant difference between groups (p-value<0.01).

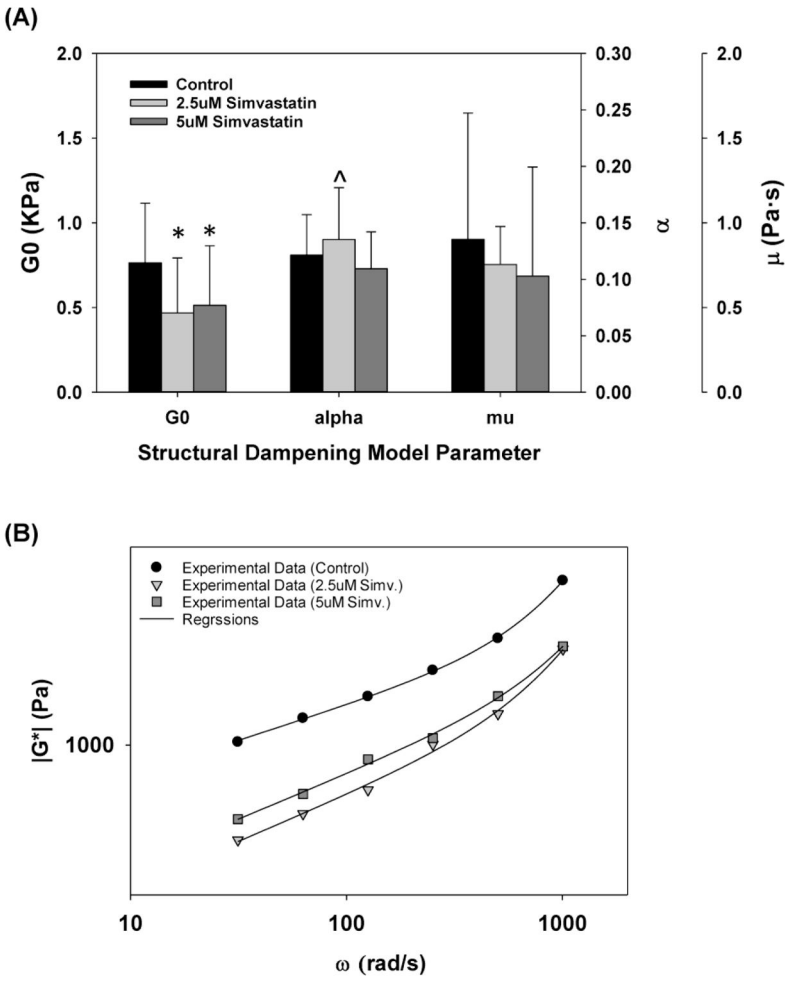

Figure 5.

Simvastatin treatment does not alter the viscoelastic properties of A549 cells (A) Changes in reference shear modulus, G_0, power law exponent, α, and Newtonian viscous damping coefficient, μ. All data are reported as median with 75/25% intervals, * indicates statistically significant difference with respect to control ($p<0.01$) and ^ indicates $p=0.03$ with respect to control. (B) Representative measurements of complex shear modulus, G* as a function of ω for cells treated with 2.5μM (triangles), 5μM (squares) and 0μM (circles, control) Simvastatin. Regression fit with structural damping equation shown in solid lines.

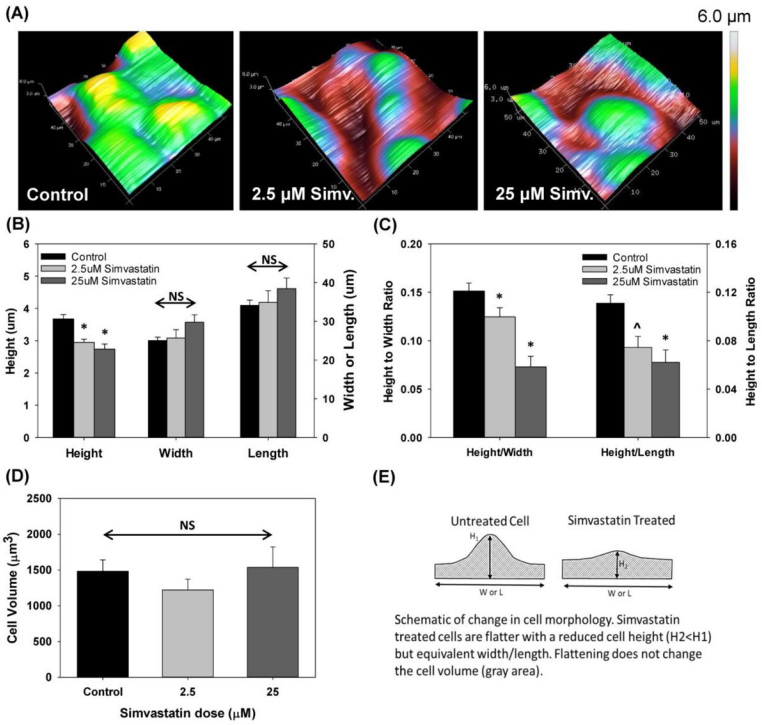

Figure 6.

Simvastatin treatment alters cellular morphology. (A) 3D surface plot of cell height as measured via AFM. (B) Measured cell height, width and length, (C) calculated height-to-width and height-to-length ratios for different Simvastatin concentrations, (D) Computed cell volume and (E) schematic representation of cell morphology variations with Simvastatin treatment. * indicates statistical difference with respect to control, $p<0.01$ and ^ indicates $p=0.065$ with respect to control. All data is mean ± SEM and n=15–42 cells.

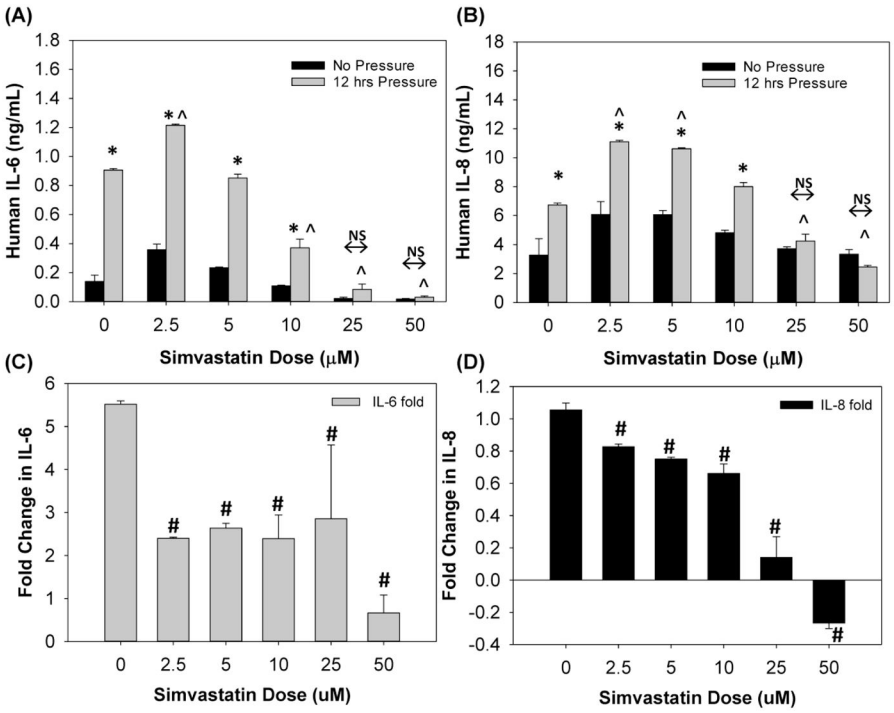

Figure 7.

Effect of Simvastatin and 12 hours of cyclic pressure on IL-6 (A) and IL-8 (B) pro-inflammatory cytokine secretion (mean ± SEM). * indicates significant difference ($p<0.01$) vs. no-pressure at each Simvastatin concentration. ^ indicates significant difference ($p<0.01$) with respect untreated control sample (0uM). (C&D) Fold increase in IL-6 and IL-8 cytokine secretion due to 12 hours of cyclic pressure as a function of Simvastatin concentration (mean ± SEM). # indicates significant difference ($p<0.05$) with respect untreated control sample (0uM).